*33rd EPS Conference on Plasma Phys. Rome, 19 - 23 June 2006 ECA Vol.**30I**, P-2.132 (2006)*

Thomson scattering analysis of large scale fluctuations in the ASDEX Upgrade edge

B. Kurzan, H. D. Murmann, C. Konz, L. D. Horton, A. Herrmann, M. Maraschek,
H. W. Müller, J. Neuhauser, A. Schmid, ASDEX Upgrade Team
MPI für Plasmaphysik, EURATOM Association, Boltzmannstr. 2, 85748 Garching, Germany

Introduction

The expulsion of heat and particles by magnetic field aligned filaments during type-I Edge Localized Modes (ELMs) was found at the low field side of ASDEX Upgrade in the steep gradient region and scrape-off layer (SOL) by 2D-Thomson scattering [1], in the far SOL by Langmuir probes [2, 3], and on limiter and divertor structures by 2D-thermography [4, 5]. With 2D-Thomson scattering it is now also possible to analyze quantitatively the large scale fluctuations of electron density and temperature in the steep gradient region at the plasma edge between ELMs. Their toroidal quasi-mode numbers are between 6 and 50 and their fluctuation level can reach up to 100%.

Experimental Setup

The vertical Thomson scattering diagnostic consists of a bundle of up to six vertically launched, radially staggered Nd-YAG laser beams. The scattered light is observed from the low-field side in 16 spatial channels with one optical detection system per channel only. This arrangement forms a vertically stretched (R, z)-matrix of scattering volumes in a poloidal cross section. The whole system was shifted radially to measure low field side edge plasma profiles and structures in the poloidal plane (Fig. 1). A 2D-snapshot of electron density and temperature structures is obtained by firing the radially staggered lasers one after the other within 2 μs, which defines the 'exposure time'. The parameters of the discharges #20414 to #20420, which are investigated in this paper, are: toroidal magnetic field $B_t = -2.7$ T, plasma current $I_p = 1.00$ MA, safety factor $q_{95} = (5 - 5.2)$, line-averaged density $\bar{n}_e = (6.4 - 8.4) \times 10^{19}$ m^{-3}, heating power by neutral beam co-injection $P_{NBI} = (5 - 10)$ MW, and by ion cyclotron resonance $P_{ICRH} = (1.3 - 1.9)$ MW, elongation

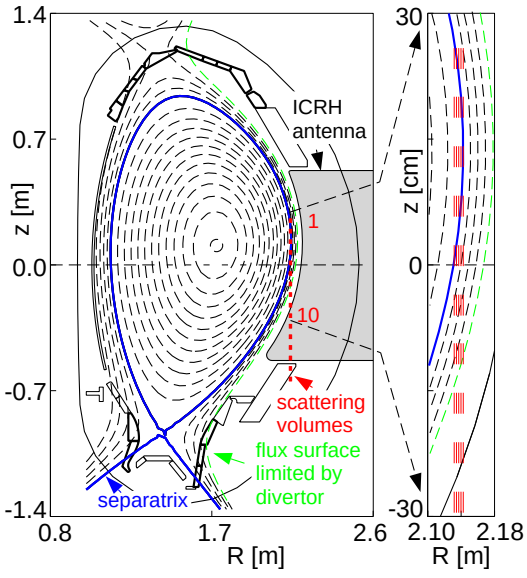

Figure 1: poloidal cross section

$\kappa = 1.76 - 1.84$, upper triangularity $\delta_u = 0.13 - 0.18$, lower triangularity $\delta_l = 0.37 - 0.38$.

Results

The 2D-structures of electron density and temperature, n_e, T_e, are plotted in (R, z)-space relative to R_{out}, the outermost position of the separatrix on the low field side, as determined by magnetics (Fig. 2a). In plots of the fluctuations Δn_e, ΔT_e, where from a single snapshot the mean over 20 snapshots is subtracted, small amplitude fluctuations between ELMs come out clearly (Fig. 2b).

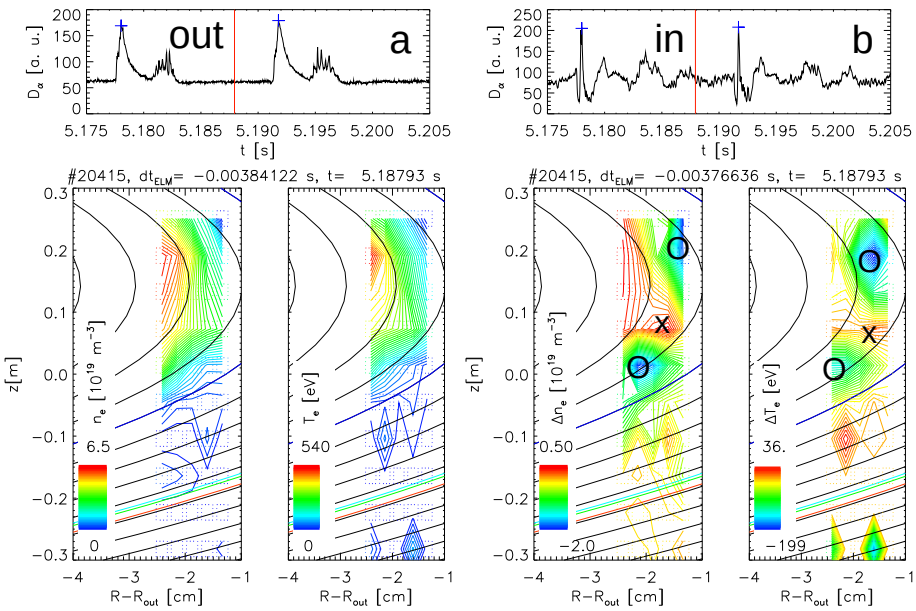

Figure 2: n_e and T_e contours (a) and fluctuation structures Δn_e, ΔT_e (b) with $n_{tor} = 13.2$ between ELMs

Assuming that the observed structures are aligned to the magnetic field, the toroidal quasi-mode number is here with [1] $n_{tor} = 13.2$. The plasma was shifted radially so that with 2D-Thomson scattering a radial region between 0 and 3 cm inside the separatrix, covering the steep gradient region, could be investigated. The width of the steep gradient region varies during ELM and inter ELM phases. This is quantified by $\langle n_e \rangle_{H5}/(dn_e/dR)$, where $\langle n_e \rangle_{H5}$ is the electron density line-integral H5 of the DCN interferometer, normalized to the integration path length inside the separatrix. The H5 line-integral includes the pedestal shoulder. dn_e/dR is the radial gradient of the electron density, determined by Thomson scattering. The relative

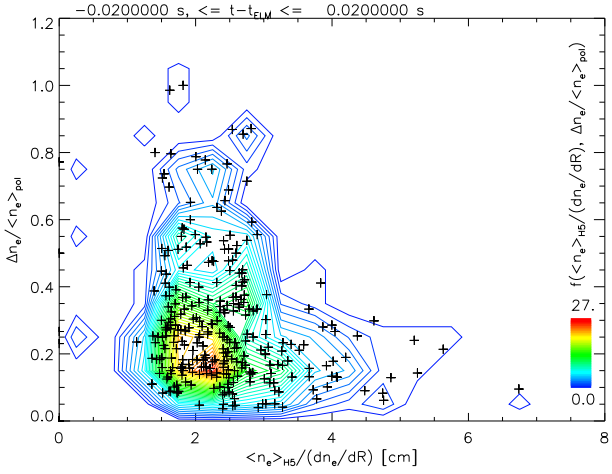

Figure 3: scaling of $\Delta n_e/\langle n_e \rangle_{pol}$ with $\langle n_e \rangle_{H5}/(dn_e/dR)$

density fluctuations $\Delta n_e/\langle n_e\rangle_{pol}$, where $\langle n_e\rangle_{pol}$ is the poloidally averaged background plasma density, determined by Thomson scattering, generally decrease with increasing width of the steep gradient region both for ELM and inter-ELM phases (Fig. 3). No clear difference between the two phases is found. The data points (symbols '+') are over-plotted here and in the following figures by the contour lines of a histogram function f indicating the frequency of the data points. For both ELM and inter-ELM phases the relative density fluctuations decrease

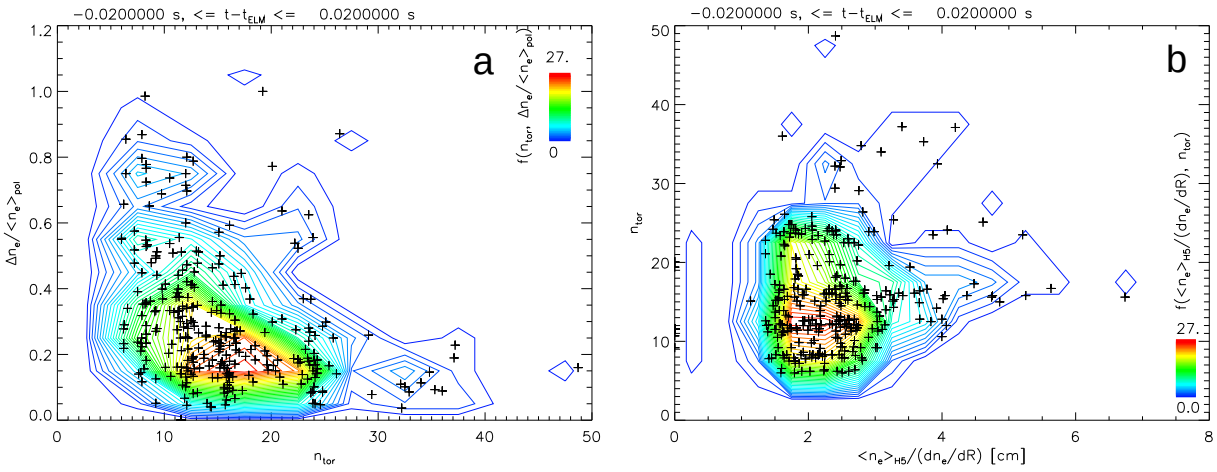

Figure 4: scaling of $\Delta n_e/\langle n_e\rangle_{pol}$ with n_{tor} (a), and of n_{tor} with $\langle n_e\rangle_{H5}/(dn_e/dR)$ (b)

with increasing toroidal quasi-mode number (Fig. 4a). For low toroidal quasi-mode numbers, $n_{tor} < 10$ the relative fluctuation amplitudes approach 1, while for the largest observed mode numbers, $n_{tor} = 40 - 50$ the relative fluctuation amplitudes are below 0.25. For a given wave number practically all relative fluctuation levels up to an upper boundary are observed, indicating that large scale fluctuations in the growing and saturated state are detected. The upper boundary of the observed toroidal mode numbers decreases with increasing widths of the steep gradient region (Fig. 4b). The most frequent mode number is around $n_{tor} \approx 12$. For widths of the steep gradient region, $\langle n_e\rangle_{H5}/(dn_e/dR) \leq 3$ cm, practically all toroidal wave numbers larger than $n_{tor} = 6$, which is the resolution limit of the diagnostic, up to an upper limit are excited. For larger widths of the steep gradient region, $\langle n_e\rangle_{H5}/(dn_e/dR) \geq 3$ cm, the lower boundary of the observed n_{tor} increases and the upper boundary decreases. The radial distributions of the relative fluctuations $\Delta n_e/\langle n_e\rangle_{pol}$ are overplotted by histogram functions, which are normalized to 1 for each radial cell (0.5 cm wide), and for each radial cell the mean values of the relative fluctuations were calculated (Fig. 5). For inter-ELM phases the relative fluctuations $\Delta n_e/\langle n_e\rangle_{pol}$ extend between 0.2 cm and 2.7 cm inside the separatrix (Fig. 5a). The maximum relative fluctuation amplitude of $\Delta n_e/\langle n_e\rangle_{pol} \approx 0.85$ is found at 1 cm inside the separatrix, while the mean values of the fluctuations have a broader maximum between 0.5 cm and 1 cm inside the separa-

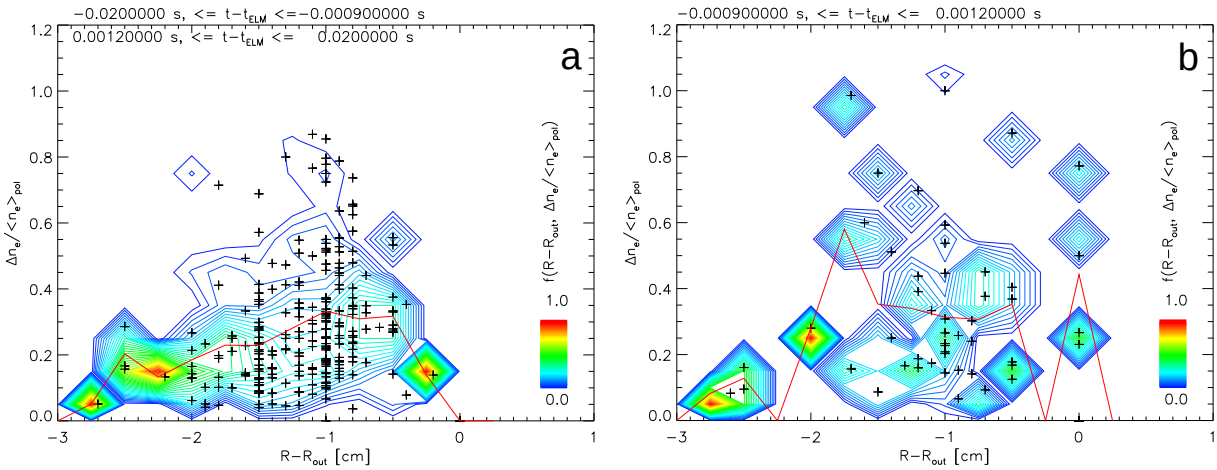

Figure 5: radial profile of $\Delta n_e/\langle n_e\rangle_{pol}$ between ELMs (a) and around ELMs (b), the red lines are the mean values for each radial cell, which is 0.5 cm wide

trix. Note that the experimentally observed single modes are much narrower than the envelopes shown in Fig. 5. For time points around ELMs the maximum relative fluctuation amplitudes reach values of $\Delta n_e/\langle n_e\rangle_{pol} \approx 1$ (Fig. 5b). The corresponding minima with zero density are then 'holes', already observed earlier [1]. Near to an ELM large relative fluctuation amplitudes are also observed at the separatrix. They are, however, difficult to catch, because in only 4 out of the investigated 300 time points such modes show up. The fluctuations of the electron temperature show in principle the same behaviour as the electron density, but with larger error bars.

Discussion

A clear identification of the type of large scale mode explaining the large scale fluctuations observed with 2D-Thomson scattering is difficult, because no theoretical model exists up to now, which can explain all the details found: The fluctuation level between ELMs can get very high, $\Delta n_e/\langle n_e\rangle_{pol} \approx 0.8-1$, but no enhanced loss of particles and energy is observed as during an ELM, as seen in the D_α-signals of Fig. 2. The fluctuation amplitudes get larger with narrower width of the steep gradient region, i.e. steeper gradients (Fig. 3) and have their maximum in the steep gradient region (Fig. 5) indicating that the observed fluctuations should be gradient driven.

References

[1] B. Kurzan *et al.*, Phys. Rev. Lett. **95**, 145001 (2005)

[2] A. Kirk *et al.*, Plasma Phys. Control. Fusion **47**, 995 (2005)

[3] H. W. Müller *et al.*, Proc. 29th EPS Conf. on Plasma Phys. and Control. Fusion **26B**, O-2.06 (2002)

[4] A. Herrmann *et al.*, Plasma Phys. Control. Fusion **46**, 971 (2004)

[5] T. Eich *et al.*, Plasma Phys. Control. Fusion **47**, 815 (2005)